ISSN NO: 2770-4491
January 2025

Synthesis Of Elements And Increased Radionuclide Activity Induced By Supersonic Spiral Jet

Kholmurad Khasanov[1], Elena Urusova[2], Rashid Eshburiev[1,*]
[1]Samarkand State University, Nuclear physics and Astronomy department of
Engineer Physics Institute, 140104, Samarkand, Uzbekistan
[2]Institute of Nuclear physics Uzbekistan Academy of Science, 100047, Tashkent, Uzbekistan
[*]Corresponding author: eshburiyev0082@gmail.com

Abstract

Intranuclear leakage of liquid protons was experimentally observed during the deceleration phase of the spiral-waved jet emitted from Kholmurad Khasanov's dynamic emitter. The gas stream from the nozzle forms supersonic spiral-type jets with spatially modulated extreme density, enhanced by shock-wave structures. In these jets, phenomena such as over-compression and over-acceleration occur, creating a high-density energy field as the internal energy of the gas or liquid decreases. The resulting instability within the jet leads to explosions accompanied by intense ultraviolet light flares. These conditions are hypothesized to promote the synthesis of new elements and increase radionuclide activity, as verified by gamma-spectrometric analysis. In the experiments, elements such as carbon, calcium, silicon, and aluminum—previously absent in the original samples—were detected on solid surfaces after exposure to the jet.

Key words: Dynamic emitter; Over-compression; Ultraviolet irradiation explosion; Synthesis of elements; Radionuclide activity; Gamma-spectrometric analysis.

1. Introduction

Understanding the properties of atomic nuclei remains a significant challenge due to the complexities of strong nuclear interactions, which resist comprehensive explanation within a single theoretical framework. Approximate models, such as the liquid drop model proposed by Bohr and Weizsäcker [1, 2], have been instrumental in explaining certain nuclear properties like incompressibility, saturation of nuclear forces, and nucleon "evaporation." This model views the nucleus as a spherical, uniformly charged liquid drop, allowing for the investigation of energy conditions for various decay modes and the development of semi-quantitative theories of heavy nuclear fission [3]. However, it falls short in explaining phenomena like the asymmetry in heavy nuclei fission [4] and the stability of "magic" nuclei [5].

Extending the liquid drop model to include surface tension, nuclear fission, and fusion led to the Weizsäcker semi-empirical formula. This formula enables the calculation of a nucleus's binding energy and mass based on its nucleon composition and proton number. Treating the nucleus as an incompressible liquid capable of deformation and fission under external and internal forces acknowledges that strong interactions are pivotal in nucleus formation, while weak interactions contribute to increased radioisotope activity [6].

The synthesis of new elements and heightened radionuclide activity suggest shifts in the balance of nuclear interactions, typically observed under critical conditions like nuclear reactions (fission, fusion, neutron bombardment) as first noted by the Joliot-Curies [7]. Notably, similar conditions may be achieved without traditional nuclear reactions—such as when matter attains a super-dense state through extreme compression or acceleration—leading to fields of super-dense energy. These conditions may manifest in supersonic high-energy jets with spiral-curled capillary structures, supported by various theoretical and experimental studies [8, 9].

In this context, Kholmurad Khasanov developed a dynamic emitter capable of detecting intranuclear leakage of liquid protons from the atomic nucleus [10]. This emitter generates a self-focusing jet using a specially designed resonant dynamic construction. A novel phenomenon was observed: a partially enlarged supersonic air jet expelling vertically upwards from a nozzle with a central cone-shaped structure formed by two intertwining spirals [11]. An extremely high-density energy field was detected in the gas flow from this nozzle, which functions both as a resonator and a dynamic emitter [12].

During episodes of over-compression and over-density in the supersonic spiral jet, high-energy electromagnetic radiation was observed [12]. In the case of a supersonic underwater jet produced by the

dynamic emitter, high-energy fields were generated in condensed media, with vapor streams creating stationary boundary layer canals that significantly compressed the jet's transverse and longitudinal sections.

Analyzing the adiabatic gas expansion within the dynamic emitter revealed a reduction in the internal energy of the jet and an increase in its kinetic energy [13]. Measurements indicated that the jet's over-compression was non-linear and accompanied by high-energy radiation due to the over-acceleration of its molecules. This phenomenon differs markedly from sonoluminescence, where light bursts result from collapsing cavitation bubbles under ultrasonic excitation.

While the study of structured jets presents many open questions, similar phenomena are noted in astrophysical jets emitted by young stellar objects [14]. These jets, found throughout the universe from protostars to supermassive black holes, are thought to originate from central objects surrounded by magnetized accretion disks [15]. Astrophysical jets often exhibit significant sub-radial structure, high Mach numbers (M~20), and can propagate over large distances without substantial energy loss or structural failure. The stellar matter in these jets accelerates in the star's gravitational field to supersonic speeds, generating shock waves that emit ultraviolet and X-ray radiation [16].

In contrast, the dynamic emitter produces structured jets that can propagate over long distances at lower Mach numbers (M = 1–3), including subsonic reactive jets. These jets generate fields of extremely high energy density and induce cooling due to reduced internal gas energy and radiation loss.

In the spiral-waved supersonic jet from the dynamic emitter, conditions conducive to proton collisions arise, increasing the likelihood of both central and non-central collisions. Each proton's surrounding electromagnetic field and associated photons may interact with other protons or nuclei, sometimes tangentially.

Experiments at facilities like the Large Hadron Collider (CERN) and the Relativistic Heavy Ion Collider (Brookhaven National Laboratory) have demonstrated that quark-gluon plasma can form incompressible, superfluid liquid drops under specific collision conditions [17, 18]. Initially observed during heavy ion collisions at energies above 200 GeV, these short-lived particles rapidly disintegrate. Subsequent experiments suggest that phase transitions can also occur with lighter particles at lower energies, raising the possibility of photon-ion collisions generating smaller quark-gluon plasma drops.

For example, when a photon collides with an ion, a quark-gluon liquid is produced, accompanied by a light explosion, leading to the expansion of the liquid in the azimuthal projection, cooling, and the formation of subatomic particles like hadrons [19]. The formation of quark-gluon liquid drops alters the nucleus, resulting in the synthesis of new elements and an increase in unstable radionuclides. These micro-drops of quark-gluon plasma are expelled during light explosions, providing direct evidence of this ephemeral state of matter (lasting 10^{-11} to 10^{-6} seconds).

Our experimental data confirm the discovery of intranuclear proton leakage during the deceleration phase of the spiral-waved jet emitted by the dynamic emitter. The high-density energy field within these jets fosters conditions favorable for synthesizing new radioactive and non-radioactive nuclides, as validated by gamma-spectrometric analyses of solid samples processed by the dynamic emitter.

2. Theoretical part

2.1. Over-compressibility of continuous medium in adiabatic approximation

The nozzle of the dynamic emitter acts as a resonator, creating stationary wave structures within continuous media. Over-compressibility and surges in over-density occur due to over-acceleration within the spiral supersonic jet. These spiral threading wave structures form stable boundary layers and emit an energy field of extremely high density, as shown in previous studies [20, 21].

The expansion process in the pre-combustion chamber does not introduce significant changes, but the parameters—such as pressure and absolute temperature—vary at different locations within the system. The behavior of the gas within each sufficiently small volume is adequately described by the adiabatic equation [13]. The expansion in the pre-combustion chamber of the dynamic emitter is considered a reversible adiabatic process.

The enthalpy and internal energy of the gas are related by the following Eq. (1):

$$h = e + pV \ , \qquad (1)$$

ISSN NO: 2770-4491
January 2025

where e – is the internal energy, h - is the enthalpy, and pV represents the pressure-volume product. The authors suggest expressing this relationship in terms of the speed of sound and the adiabatic index, as shown in Eq. (2):

$$h = e + pV = \frac{a^2}{(\gamma - 1)} = \frac{a^2}{\gamma(\gamma-1)} + \frac{a^2}{\gamma}. \quad (2)$$

Here γ - is the adiabatic index, $e = \frac{a^2}{\gamma(\gamma-1)}$, $h = \frac{a^2}{\gamma-1}$, $\frac{a^2}{\gamma} = pV$.

The phenomenon of over-compressibility and surges in over-density arises due to a decrease in internal energy and a corresponding increase in kinetic energy within the conical cross-section of the pre-combustion chamber during adiabatic gas expansion. This leads to enhanced intermolecular interaction forces and high molecular acceleration, resulting in over-compressibility both at the outlet aperture and in the jets that propagate over long distances without significant energy loss or structural failure.

The intermolecular interaction forces transport accelerated molecules over short distances, but the molecules themselves experience acceleration values of up to 10^{14}-10^{16} m/s^2 [11, 21], which leads to the creation of an electromagnetic energy field with extremely high density.

2.2. Boundary conditions in resonator – chamber of dynamic emitter

In our initial experiments, we generated an energy field of extremely high density near subsonic and supersonic non-enlarged underwater jets emerging from the dynamic emitter [10], which featured a nozzle with a conical central body. The detailed construction is shown in Figure 1. The length of the generated wave structure was approximately 10 times the diameter of the nozzle's outlet. The nozzle was constructed using bronze and other metals, while for water injectors, composite materials or metamaterials such as textolite were used.

The nozzle design (Figure 1) allows for longitudinal displacement of the central conical body (1) within the truncated cone (2), enabling precise positioning of its tip relative to the nozzle's exit section. We performed gas-dynamic and energetic investigations using various configurations of non-enlarged underwater jets under different operational conditions and dimensional parameters.

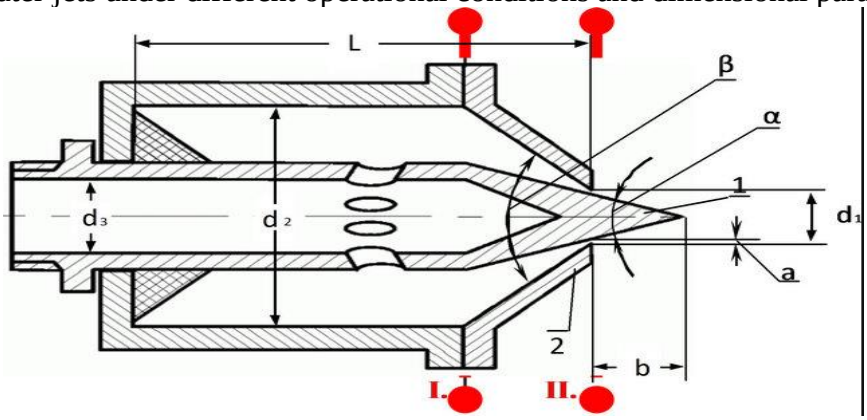

Fig.1. Construction of dynamic emitter with central cone. Here: 1 – is central cone with diameter d_3 = 25 mm and angle α = 30; 2 – is truncated cone of pre-combustion chamber with diameter d_2 = 60 mm and angle β = 60; d_1 – is diameter of nuzzle outlet aperture; circular gap, a = 0.3 – 0.6 mm; external part of internal cone, b = 3 - 6 mm; length of pre-combustion chamber, L = 150 mm [10].

The optimal conditions for the interaction of subsonic and supersonic jets were outlined in [10]. These experiments were conducted in gases, with variable gas pressure and different pre-combustion chamber geometries. A compressor provided filtered gas at pressures ranging from 1.5 to 31 atmospheres. When the gas was released into the atmosphere, it formed a highly compressed stream of spiral twisted irradiating wave structures, consisting of cells with defined dimensions [12].

In [10], it was shown that 73% of the increase in kinetic energy in section II-II was due to a decrease in the internal energy of the gas. This increase in kinetic energy was accompanied by a corresponding decrease in internal energy and a drop in temperature. The sound velocity reached critical levels in the cross-section. Computations indicated that the contribution of internal energy to the jet's kinetic energy exceeded the photoelectric energy by more than three times.

ISSN NO: 2770-4491
January 2025

Thus, the phenomena of over-compressibility, over-density surges, and the generation of a high-density energy field occur in both non-enlarged underwater and gas jets emerging from the dynamic emitter, driven by the decrease in the internal energy of the continuous medium.

2.3. Estimate of over-acceleration

To estimate over-acceleration, a model of hard elastic spheres and correction factors based on Van der Waals forces was used [13]. The interaction potential is defined as follows (3):

$$\varepsilon(r) = \begin{cases} \infty, & r < 2 \cdot r_S \\ -\frac{\beta}{r^m}, & r \geq 2 \cdot r_S \end{cases} . \quad (3)$$

Here r_S– is the cross-sectional radius of gas molecule collisions, and the best approximation is achieved with m = 6. The parameter β is expressed in terms of Avogadro's number N_A and the Van der Waals coefficients *a* and *b* as follows (4):

$$\beta = \frac{9ab}{4\pi \cdot N_A^3} \quad (4)$$

All parameters for certain gases are provided in [13].

The critical volume V_{crit} is is given by equation (5), and the cross-sectional radius can be determined using Eq. (6):

$$V_{crit} = 16\pi \cdot N_A \cdot r_S^3 \quad (5)$$

$$2r_S = \sqrt[3]{\frac{V_{crit}}{2\pi \cdot N_A}} \quad (6)$$

The force responsible for over-acceleration is derived from the interaction potential as follows (7):

$$F = -\frac{d\varepsilon}{dr} = -\frac{m\beta}{r^{(m+1)}} \quad (7)$$

The acceleration can then be calculated using this force and the mass of the molecule. Heavy free ions, such as (OH^-) and (N_2^+), which arise in the jet channels, acquire significant relative accelerations.

Previous research [20, 21] has shown that the attractive force between oxygen molecules is approximately 18.9×10^{-11} N, and the acceleration of an oxygen molecule can reach 3.57×10^{14} m/s^2. For hydrogen molecules, the acceleration can be as high as 1.2×10^{16} m/s^2. Such high accelerations are the cause of gas over-compressibility and the resulting structural disruption. The over-accelerations are a direct consequence of the internal energy decrease during adiabatic gas expansion in regions of over-compression within continuous media.

3. Experimental part

3.1. Interaction of supersonic jet from the dynamic emitter with matter. Ultraviolet explosion

The experiments were conducted using the dynamic emitter (Fig. 1) to produce a non-completely enlarged underwater jet, which was expelled from the central conical nozzle (CCN). A key feature of the CCN is that the central cone protrudes from the nozzle exit. The setup allowed for the longitudinal movement of the central cone [10].

In our experiments, air and vapor-air jets formed channels with stationary boundary layers, undergoing heavy compression in both transverse and longitudinal cross-sections. For instance, when the diameter of the nozzle exit was 3 mm, the over-compressibility of the jets was observed up to a range of 30 mm. This unexpected spiral-twisted configuration of the jet may have various practical applications and could lead to new goals in the field of gas dynamics for further theoretical understanding. Jets with such configurations introduce a new type of vortex flow [11].

Schlieren photography and laser visualization enabled us to detect previously unknown spiral-curled, self-focusing structures in supersonic and hypersonic jets. Over-compression in the ultraviolet range within these jets generated powerful light explosions (Figs. 2b, c), characterized by high-frequency waves and significant over-compressibility [11–13].

ISSN NO: 2770-4491
January 2025

Fig.2. a) Interaction of supersonic jet with a solid body, leading to the formation of cool plasma and new elements; b) A powerful explosion of light in the white, yellow, and red spectrum ranges; c) Light explosion visible in the red, violet, turquoise regions of the spectrum.

Air under a pressure range of 2 to 6 bar was fed into the dynamic emitter, producing a supersonic jet (Fig. 2a). Interaction of this jet with low-temperature plasma formed from the combustion products of hydrocarbons (such as methane and propane) triggered powerful explosions of ultraviolet radiation (Fig. 2c). These explosions appeared to occur within nanometer-sized local volumes in vacuum spaces inside matter, such as atoms, nanopores, cracks, and capillaries. The explosions resulted in nuclear fission and the fusion of new elements and compounds with a porous structure.

The phenomenon of artificial radioactivity, described by Frederic and Irene Joliot-Curie [22, 23], involved the synthesis of new radioactive isotopes via neutron bombardment as a result of nuclear fission reactions. However, to date, there has been no data on the fusion of radioactive and non-radioactive isotopes without neutron involvement.

In our experiments, we observed the generation of radioactive isotopes due to the interaction of the supersonic jet with solid body targets. The fusion of nuclides, including silicon (Si), aluminum (Al), and calcium (Ca), and the increase in radionuclide activity (e.g., radium (Ra), thorium (Th), and potassium (K)) occurred within the jet without external initiation of nuclear interaction. Both stable and unstable radioactive nuclei were formed, and the activity of the resulting radioisotopes increased.

The analysis of the samples (targets) subjected to the supersonic jet of the dynamic emitter was conducted using a SNOL muffle furnace, OHAUS PA 214C electronic analytical balance, VIT 2 hydrometer, and a KFK photo-electronic colorimeter between March and December 2020. Spectra of the powerful ultraviolet light explosions were recorded in capillary supersonic jets (Fig. 3a). Additionally, a comparison between experimental data and computer simulations of the ultraviolet explosion spectra was made (Fig. 3b).

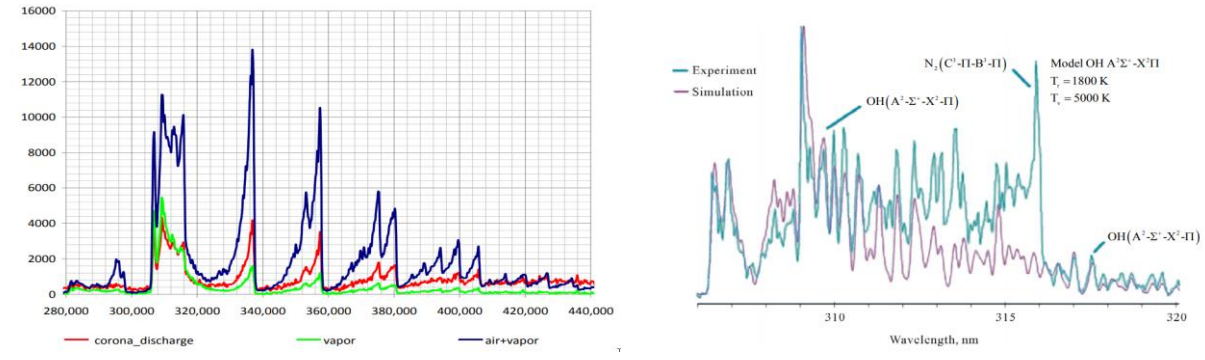

a b

Fig.3. a) Spectrum of the powerful ultraviolet explosion in a capillary supersonic jet; b) Comparison of the experimental and simulated spectra of ultraviolet flashes.

3.2. Synthesis of new elements and compounds

The interaction of the spiral-twisted supersonic jet, accompanied by phenomena of over-compression and over-acceleration, as well as the formation of cool condensed plasma on the surface of a solid body, resulted in the fusion of isotopes and the synthesis of new elements not initially present in the substrate. On a silicon

ISSN NO: 2770-4491
January 2025

substrate (Fig. 5a), the synthesis of carbon and other elements occurred. Spectrum analysis was carried out on both the initial and modified samples.

In addition to carbon synthesis on the silicon substrate, the synthesis of chlorine (Cl), calcium (Ca), sodium (Na), and zinc (Zn) in the presence of argon ions was also detected, as shown in Table 1.

Table 1 Elemental composition of initial and final Samples

Sample Area	Element	Final Weight %	Initial Weight %
1	Cl	0.45	0.0080
	Ca	36.22	0.0013
2	Na	0.45	0.0033
	Cl	1.92	0.0080
	Ca	49.21	0.0013
	Zn	1.61	0.00006

In another set of experiments, samples with different initial compositions and densities (Samples 1, 2, and 4) were studied alongside a modified sample (Sample 3), which had been subjected to the dynamic emitter jet. The results, presented in Table 2, show a significant increase in the mass fraction of silicon oxide (SiO_2) and a corresponding decrease in the mass fraction of iron oxide (Fe_2O_3).

Table 2 Diagnostic results of oxides and ash mass fractions, and samples volume density in g/cm^3.

Parameters	Sample 1 Source material	Sample 2 Source material	Sample 3 final material	Sample 4 Source material
Mass fraction of SiO_2, (%)	2.1	33.38	82.92	35.24
Mass fraction of Fe_2O_3 (%)	2.50	5.00	1.50	3.90
Mass fraction of Al_2O_3 (%)	1.00	33.41	11.24	25.00
Ash content (%)	7.0	-	-	-
Density (g/cm^3)	0.83	2.68	1.00	2.78

3.3. Increasing of radionuclides activity

Investigations were conducted on carbon and silicon samples, both in their initial state and after being processed by the supersonic jet of the dynamic emitter. The results of gamma-spectrometric examinations are presented in Tables 3 to 5. The testing was performed at the Tashkent Institute of Nuclear Physics using a CANBERRA gamma-spectrometer (detector GC2018, analyzer DSA-1000, with an exposure time of 3600 seconds).

Table 3. Gamma-spectrometric results for initial and processed carbon samples.

Nuclide	Activity (Bq)	Random error (%)	Specific activity (Bq/kg)	Absolute error (Bq/kg)	Relative error, (%) (P=0.95)
Initial carbon sample					
Ra-226	< 5.0985	-	< 25.12	-	-
Th-232	< 3.3829	-	< 16.66	-	-
K-40	37.434	0.23	184.41	52	28.1
Processed carbon sample					
Ra-226	7.3989	0.12	30.867	5.5	17.9
Th-232	8.3852	0.05	34.982	3.9	11
K-40	164.1	0.01	684.61	64	9.39

From the data in Table 3, it is clear that the activities of Ra-226, Th-232, and K-40 significantly increased after the impact of the supersonic jet from the dynamic emitter.

In Table 4, we see a considerable increase in the activities of Ra-226 and K-40, while the activity of Th-232 remains practically unchanged after processing.

ISSN NO: 2770-4491
January 2025

Further investigations were conducted on initial Sample 0 and processed Samples 1, 2, and 3. These samples were also analyzed using the CANBERRA gamma-spectrometer (detector GC2018, analyzer DSA-1000).

Table 4. Gamma-spectrometric results for initial and processed silicon samples.

Nuclide	Activity (Bq)	Random error (%)	Specific activity (Bq/kg)	Absolute error (Bq/kg)	Relative error (%) (P=0.95)
Initial silicon sample					
Ra-226	26.01	0.17	260.1	54	20.6
Th-232	< 3.4024	-	< 34.02	-	-
K-40	53.214	0.34	532.14	220	40.8
Processed silicon sample					
Nuclide	Activity, Bq	Random error,%	Specific activity, Bq/kg	Absolute error, Bq/kg	Relative error,% (P=0.95)
Ra-226	47.394	0.14	473.94	79	16.7
Th-232	< 3.5418	-	< 35.42	-	-
K-40	112.29	0.23	1122.9	310	27.8

Table 5. Consolidated report on nuclide identification in samples 0, 1, 2, and 3.

IDENTIFICATED NUCLIDES					
Nuclide	Identification validity	Energy, (keV)	Output (%)	Activity (Bq/g)	Error
Sample					
0 K-40	0.982	1460.82*	10.55	1.92773E-002	1.86540E-002
0 Pb-212	0.999	238.63*	43.60	3.28541E-003	1.99991E-003
0 Bi-214	0.666	609.31*	45.49	9.83763E-004	2.32812E-003
1 K-40	0.980	1460.82*	10.55	3.288E-001	4.384E-002
2 K-40	0.985	1460.82*	10.55	5.575E-001	5.258E-002
3 K-40	0.932	1460.82*	10.55	5.147E-001	4.623E-002
1 Tl-208	0.428	583.19*	85.00	1.207E-002	2.206E-003
2 Tl-208	0.419	583.19*	85.00	1.572E-002	1.857E-003
3 Tl-208	0.428	583.19*	85.00	1.401E-002	1.674E-003
1 Pb-212	0.992	238.63*	43.60	2.146E-002	3.006E-003
2 Pb-212	0.994	238.63*	43.60	3.097E-002	3.317E-003
3 Pb-212	0.987	238.63*	43.60	3.872E-002	2.649E-003
1 Bi-214	0.716	609.31*	45.49	2.408E-002	3.639E-003
2 Bi-214	0.706	609.31*	45.49	2.113E-002	3.688E-003
3 Bi-214	0.715	609.31*	45.49	2.533E-002	3.782E-003
1 Ac-228	0.506	911.20*	26.20	2.690E-002	7.604E-003
		968.96*	15.90	2.387E-002	1.248E-002
2 Ac-228	0.581	338.32*	11.40	3.669E-002	1.012E-002
		911.20*	26.20	3.852E-002	6.523E-003
3 Ac-228	0.986	338.32*	11.40	3.815E-002	9.055E-003
		911.20*	26.20	3.142E-002	6.403E-00

From the consolidated report in Table 5, it is evident that the activity of K-40 increased by approximately 30-50 times, Pb-212 increased by about 10 times, and Bi-214 increased by approximately 20-25 times after the jet processing.

Table 6 Specific activity of radionuclides in mineral powder samples

№	Radionuclide	Specific activity, A±Δ (Bq/kg)	
		Sample №1 (S-0012-20G) initial	Sample №2 (S-0001-21G) processed

1	Ra-226*	3.4±1.2	32.8±0.9
2	Th-232**	4.9±1.1	27.4±1.3
3	K-40	19.3±3.5	307.3±35.6

* - activity of radionuclide Ra-226 calculated on base of daughter radionuclides Pb-214, Bi-214 activity;
**- activity of radionuclide Th-232 calculated on base of daughter radionuclides Tl-208, Pb-212, Ac-228 activity.

From the data in Table 6, the activity of Ra-226 increased by 9.7 times, Th-232 increased by 5.6 times, and K-40 increased by 5.9 times. This suggests the synthesis of radioactive nuclides under the conditions created in the supersonic jet of the dynamic emitter due to over-compression, over-acceleration, and the generation of high-density energy fields, resulting from the decrease in the internal energy of the continuous medium.

5. Conclusions

In this study, we have experimentally demonstrated that the gas stream emitted from the nozzle of a dynamic emitter forms a supersonic double spiral jet with spatially modulated extreme density due to shock-wave structures. The instabilities within these jets lead to explosions accompanied by powerful flashes of ultraviolet light.

Our findings reveal that the interaction of these supersonic spiral jets with solid surfaces can result in nuclear fusion, leading to the formation of new elements such as carbon, calcium, silicon, aluminum, and others—elements that were not present in the original samples. Similar results were observed in experiments utilizing ion beams of inert gases, which also facilitated the synthesis of new elements.

Moreover, the explosions following the ultraviolet flashes in the supersonic jets were found to result in increased radionuclide activity. This was confirmed through gamma-spectrometric analysis, indicating the synthesis of both radioactive and non-radioactive nuclides. The dynamic emitter, therefore, may function as a miniature microtron, enabling the synthesis of radionuclides for both fundamental research and practical applications.

Overall, our work provides new insights into the synthesis of elements and the enhancement of radionuclide activity induced by supersonic spiral jets. The phenomena of over-compressibility and over-acceleration within these jets, along with the generation of high-density energy fields resulting from the decrease in internal energy of the continuous medium, play crucial roles in these processes. This research opens up new possibilities for the synthesis of radionuclides and contributes to our understanding of nuclear interactions under extreme conditions.

Acknowledgement

The authors would like to express their sincere gratitude to Prof. Leonid Dmitrievich Blokhintsev for his valuable discussions on the theoretical and fundamental aspects of this research, and to Dr. Anri Amvrosimovich Rukhadze for his repeated consultations on issues related to plasma physics.

Special thanks are extended to Dr. Muhammad Salimov, head of the Nuclear Analytics Laboratory at the Institute of Nuclear Physics of the Academy of Sciences of the Republic of Uzbekistan, for his team's detailed and thorough registration and determination of radionuclide activity.

The authors are also deeply grateful to Prof. Nikolai Gavrilovich Chechenin for his collegial discussions of the results and for repeatedly organizing seminars at the Department of Atomic Nuclear Physics of the Institute of Nuclear Physics at Moscow Lomonosov State University. Finally, we would like to thank Prof. Vladimir Savinov, from the Physics Department of Lomonosov State University, for his insightful discussions of the results and for providing materials related to radionuclide activity.

References

1. Bohr, N., Wheeler, J.A.: The mechanism of nuclear fission. Physical Review. **56**, 426 (1939).
2. Weizsäcker, C.F. v: Zur theorie der kernmassen. Zeitschrift für Physik. **96**, 431 (1935).
3. Itkis, M.G., Vardaci, E., Itkis, I.M., Knyazheva, G.N., Kozulin, E.M.: Fusion and fission of heavy and superheavy nuclei (experiment). Nuclear Physics A. **944**, 204 (2015).
4. Wilkins, B.D., Steinberg, E.P., Chasman, R.R.: Scission-point model of nuclear fission based on deformed-shell effects. Physical Review C. **14**, 1832 (1976).
5. Mayer, M.G.: On closed shells in nuclei. II. Physical Review. **75**, 1969 (1949).

6. Bethe, H.A., Bacher, R.F.: Nuclear physics A. Stationary states of nuclei. Reviews of Modern Physics. **8**, 82 (1936).
7. Lauritsen, Cc.C., Crane, uHR, Harper, W.W.: Artificial production of radioactive substances. Science. **79**, 234 (1934).
8. Foster, J.M., Wilde, B.H., Rosen, P.A., Perry, T.S., Fell, M., Edwards, M.J., Lasinski, B.F., Turner, R.E., Gittings, M.L.: Supersonic jet and shock interactions. Physics of Plasmas. **9**, 2251 (2002).
9. Hietala, H., Laitinen, T. V, Andréeová, K., Vainio, R., Vaivads, A., Palmroth, M., Pulkkinen, T.I., Koskinen, H.E.J., Lucek, E.A., Rème, H.: Supermagnetosonic jets behind a collisionless quasiparallel shock. Physical Review Letters. **103**, 245001 (2009).
10. Khasanov, K., Petukhov, S. V: Dynamic emitter. PF patent. (1996).
11. Khasanov, K.: Bi-Spiral Switched Supersonic Jet Flow Escaping from a Circular Nozzle: Interaction with Metal and Polymer Screens, Infrared Radiation Phenomenon. In: *International Conference: Fluxes and Structures in Fluids. Physics of Geospheres*. , Moscow (2009).
12. Khasanov, K.: Visualization of super-compressibility in supersonic spiral-twisted jets. Physics Letters A. **376**, 748 (2012).
13. Khasanov, K.: Super-Compressibility Phenomenon. Journal of Modern Physics. **4**, 200 (2013).
14. McNamara III, W.B., Didenko, Y.T., Suslick, K.S.: Sonoluminescence temperatures during multi-bubble cavitation. nature. **401**, 772 (1999).
15. Mohseni, K., Colonius, T., Freund, J.B.: An evaluation of linear instability waves as sources of sound in a supersonic turbulent jet. Physics of fluids. **14**, 3593 (2002).
16. Savin, D.W., Brickhouse, N.S., Cowan, J.J., Drake, R.P., Federman, S.R., Ferland, G.J., Frank, A., Gudipati, M.S., Haxton, W.C., Herbst, E.: The impact of recent advances in laboratory astrophysics on our understanding of the cosmos. Reports on Progress in Physics. **75**, 36901 (2012).
17. Nagle, J.L., Adare, A., Beckman, S., Koblesky, T., Koop, J.O., McGlinchey, D., Romatschke, P., Carlson, J., Lynn, J.E., McCumber, M.: Exploiting intrinsic triangular geometry in relativistic he 3+ au collisions to disentangle medium properties. Physical Review Letters. **113**, 112301 (2014).
18. Huang, S., Collaboration, P.: Measurements of elliptic and triangular flow in high-multiplicity 3He+ Au collisions at sNN= 200 GeV. Nuclear Physics A. **956**, 761 (2016).
19. Aad, G., Abbott, B., Abbott, D.C., Abed Abud, A., Abeling, K., Abhayasinghe, D.K., Abidi, S.H., AbouZeid, O.S., Abraham, N.L., Abramowicz, H.: Two-particle azimuthal correlations in photonuclear ultraperipheral Pb+ Pb collisions at 5.02 TeV with ATLAS. Physical Review C. **104**, 14903 (2021).
20. Khasanov, K.: Radiation of bi-spiral switched supersonic jet flow escaping from an annular nozzle. Fluxes and Structures in Fluids. Physics of Geospheres–2009 (Abstracts), Moscow. (2010).
21. Khasanov, K.: PHENOMENA TAKING PLACE AT THE ATOMIC LEVEL UNDER CERTAIN PERTURBATIONS. In: *Abstracts of 56th International Symposium on Molecular Spectroscopy*. Ohio State University, Columbus (2001).
22. Joliot-Curie, I., Joliot, F.: Artificial production of radioactive elements. Nobel Lectures in Chemistry (1922–1941). **2**, 366 (1935).
23. Fermi, E., Amaldi, E., D'Agostino, O., Rasetti, F., Segrè, E.: Artificial radioactivity produced by neutron bombardment. Proceedings of the Royal Society of London. Series A, Containing Papers of a Mathematical and Physical Character. **146**, 483 (1934).